The Institute of Space and Astronautical Science
Report SP No. 3, March 1985

Interactions of Vortices*

By

Yuko OSHIMA

(January 10, 1985)

Summary: Interaction of vortex filaments are one of the elementary process taking place in turbulent flow, and some interesting interaction phenomena among them are studied. Firstly, several vortex rings are ejected in series along the same axis into still air through a circular orifice and the interactions of them are experimentally analyzed together with the simple numerical simulation by micro-computer using discrete vortex method in which each vortex is represented by seven vortex filaments. Secondly, an elliptic vortex ring is ejected through an elliptic orifice and the deformation of the ring due to the self interaction is followed. Thirdly, two vortex rings are ejected simultaneously from two identical circular orifices separated with a certain distance and their merging, splitting and interchanging are observed.

§I. INTRODUCTION

Study of vortex motion and the interation is one of the fascinating problem in fluid dynamics and have a long history since the works of J. J. Thomson [*1*]. During the middle of 1960s, the dynamics of vortices together with the instability of the vortex filament has attracted the interests of the fluid dynamists in connection with the investigation of turbulence, since the motion of vortices are considered as elementary process of turbulent flow [2]–[5].

Experimental investigations of the vortex rings and their interactions have been carried out also since 1970s [*6*]–[*13*]. Among them, especially the following three problems are interesting. They are passing through game of two co-axial vortex rings, deformation of elliptic vortex rings and the crosslinking of vortex filaments caused by the two vortex rings proceeding side by side along the parallel axes. These two phenomena were observed and examined in the flow with relatively low Reynolds number. Also, the measurements of the velocity and vorticity fields for turbulent vortex rings were carried out using hot wire anemometer and conditional sampling and ensemble averaging of the data and the structure of the vortex core and its decay were investigated [*14*]–[*16*].

Considering these background, these three kinds of the vortex interaction phenomena are studied experimentally as well as numerically in this paper. The first one is the interaction of vortex rings succeeively ejected along an axis. The vortex rings are

* Ochanomizu University.

formed by ejecting a certain amount of gas through a circular orifice for specified duration using a quick acting valve. The number of vortex rings formed depends on the opening time of the valve. A series of vortex rings proceed along the axis changing their travelling speeds and diameters due to their interactions with each other. The phenomena are simulated numerically by discrete vortex method in two dimensional case and time dependent variation of each discritized vortex is followed. The second is the deformation of the elliptic vortex in which the translational speed is different depending on the curvature. The last one is the crosslinking of vortex filaments by two vortex rings ejected simultaneously from two circular orifices. These two rings became closer and are connected each other into one distorted ring and then it splits again into two rings. The crosslinking of vortex filaments occurs twice in this process.

Section 2 is devoted to the experimental studies of the vortex rings. The experimental set-up and measuring method are described in §2.1 and the experimental results including the visualization pictures of co-axial vortex rings are in §2.2 and those of elliptic vortices and of crosslinking are in §2.3 and §2.4, respectively. Section 3 treates the numerical studies. The merging phenomena of some sets of vortex pair representing by the discritized vortex filaments are treated in two dimensional case. Time sequence of their distribution patterns is followed and compaired with the experiment.

The same coordinate system is used both in experimental and numerical studies, the origins are taken at the center of the orifice in the first and the second case, and at the center of the two vortex rings in the third case. The X-axis is in the proceeding direction of the ring, the R-axis is taken radially from the X-axis in the former case and Y- and Z-axes are taken perpendicularly to the X-axis each other in the last case. The Reynolds number Re is defined as $Re=vD/\nu$ where v is the translational velocity of the initially ejected vortex rings, D is the diameter of the orifice, and ν is the kinematic viscosity of the fluid.

§II. Experiment of Vortex Interaction

2.1 Experimental set-up and measuring method

Schematic diagram of the appratus is shown in Fig. 1. A certain amount of carbon dioxide gas is fed through a quick acting valve from CO_2 bottle and ejected into calm surroungings through a circular orifice with the diameter D. The CO_2 gas is used so as to visualize the flow field by schlieren method. The ejected gas forms a series of vortex rings, the number of which is controlled by the opening time of the quick acting valve, which is ajustable from 1 to 50 ms. The flow field is placed at the center of the schlieren system where the parallel light beam of strobo flash passes. The strobo light is triggered by the dealyed signal from the time instant when the quick acting valve is activated. The vortices are created under various conditions, such as the diameter of the orifice or the opening duration of the valve. Also the speed of vortex rings depends on the pressure of the reservior, which is kept constant at 1.3 atmospheric pressure throughout the experiment in order to keep the flows laminar. Series of photographs are taken at various delay time using a motor driven camera. As the reproducibility of the observed results is very good, the pictures at different events with a series of delay times are used

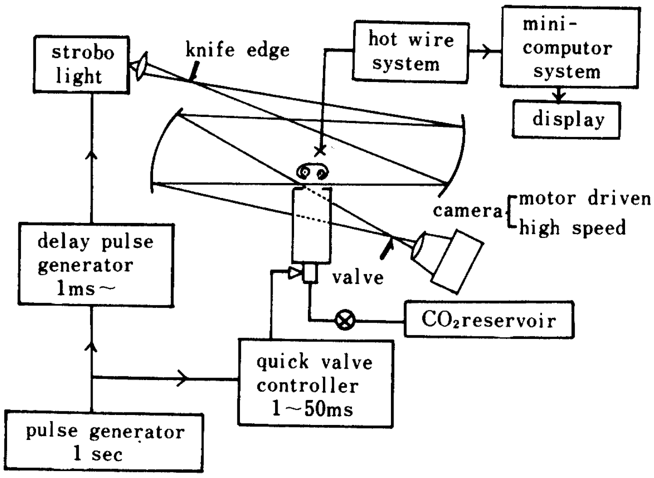

Fig. 1. Schematic diagram of the experimental apparatus.

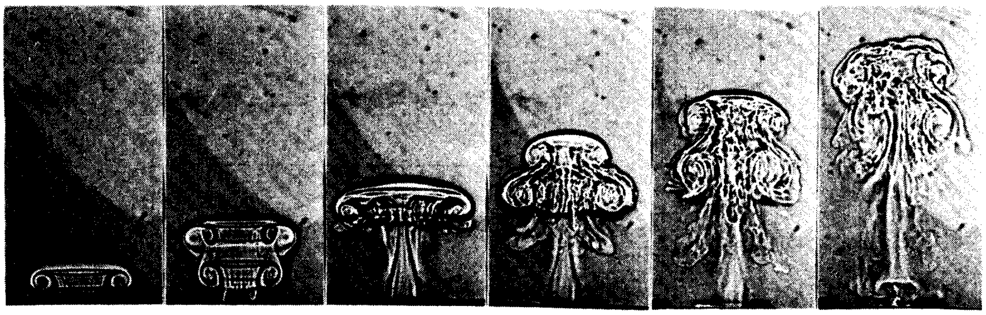

Fig. 2. A series of photographs of the vortex rings ejected from the circular orifice, $D=20$ mm, $\Delta T=5$ ms, delay time $t=5$, 9, 13, 17, 21 and 27 ms, respectively.

to get the pictures of time development of a vortex ring. Also a high speed 16 mm movie camera of 5800 flames per second is used to record the time sequence of the flow field.

As well as the circular ring, single elliptic vortex ring is generated through an elliptic orifice with the duration time of the acting valve of 1 ms. The ratios of the major and the minor radii of the orifice are 1.5:1 and 4:1.

The similar method is used for the case of two vortex rings along parallel axes. The two identical orifices have the diameter of 13 mm, and the distance of their centers is 21 mm. The distance is very critical for the flow characters and was chosen as above. If it is shorter, the crosslinking takes place too quickly to observe, and if it is larger, it occurs too late or does not occur, at all. In this case, two series of pictures are taken at each delay time from the two directions perpendicular with each other, ($X-Y$, $X-Z$ plane). It is impossible to take a top view of the vortex ring ($Y-Z$ plane), because the optical path is deterred.

2.2 Co-axial vortex rings

A series of pictures of the interactions of two co-axial vortex rings made by the orifice with the diameter of 20 mm for the valve opening time of 5 ms are shown in Fig. 2, and the Reynolds number based on the initial velocity of the first ring *Re* is about 4000. Two vortex rings are formed and play the passing through game, changing both of their translational speeds as well as the diameters, and eventually they merge into one big vortex blob. This process is clearly seen on the $X-R$ diagram shown in Fig. 3, in which the center positions of the vortex rings are plotted against the time. In these figures, their positions are marked by the same symbol for the same time instant. The diameter of the first ring increases due to the influence of the second ring, and its speed slows down. On the other hand, the diameter of the second ring decreases causing the increase of its translational velocity. Then the second one comes close to the first one, and passes through the center part of the first one. Thus one cycle of the game of passing through completes within a short time of about 40 ms. During this process, both rings become more turbulent and eventually they merge into one vortex blob as shown in the $X-T$ diagram of Fig. 4. Figure 5 shows the interaction of eight vortex rings created by a

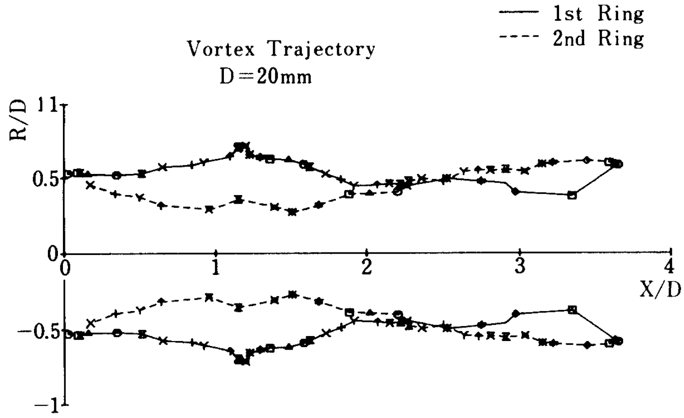

Fig. 3. $X-R$ diagram of two vortex rings, shown in Fig. 2. The same marks denote the positions of the rings at the same instant. $T=5$ ms, Rev=4000.

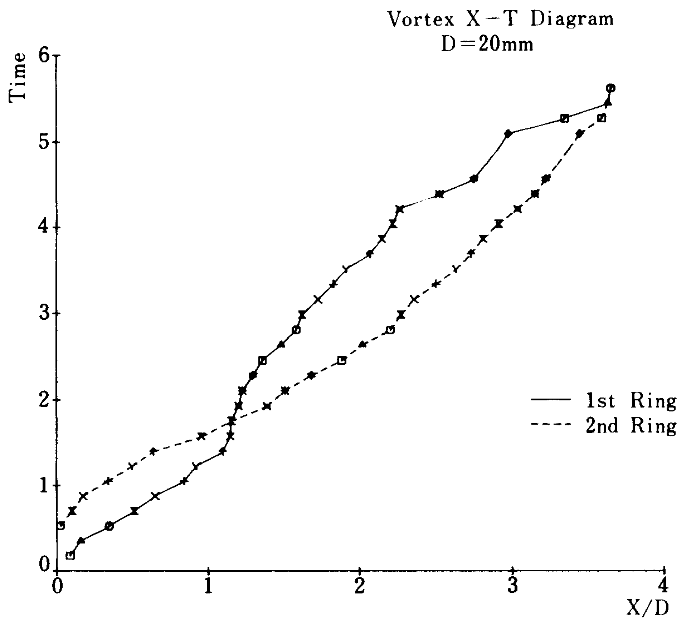

Fig. 4. $X-T$ diagram of two vortex rings, shown in Fig. 2. After one cycle of passing through game, they merge into one blob.

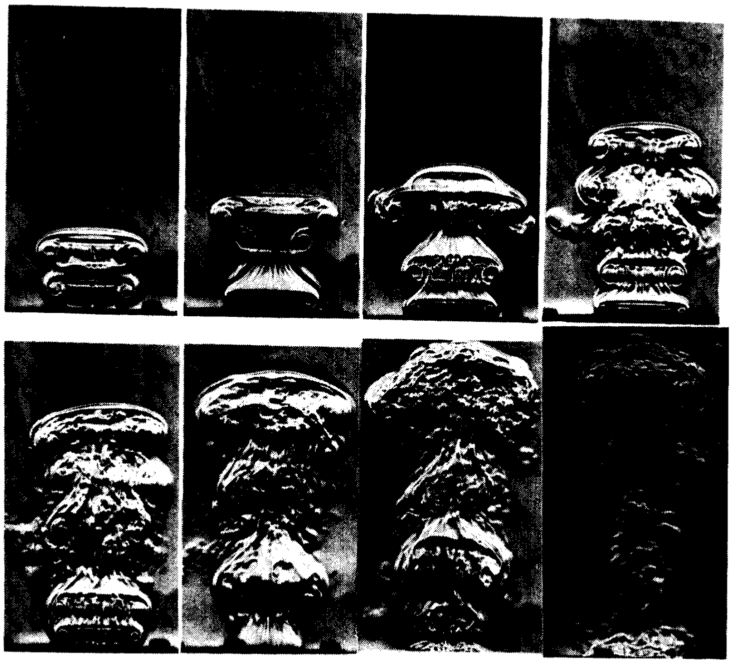

Fig. 5. A series of photographs of vortex rings ejected successively, $D=20$ mm, $\Delta T=20$ ms, delay time $t=8$, 11, 14, 17, 21, 27 and 38 ms, respectively.

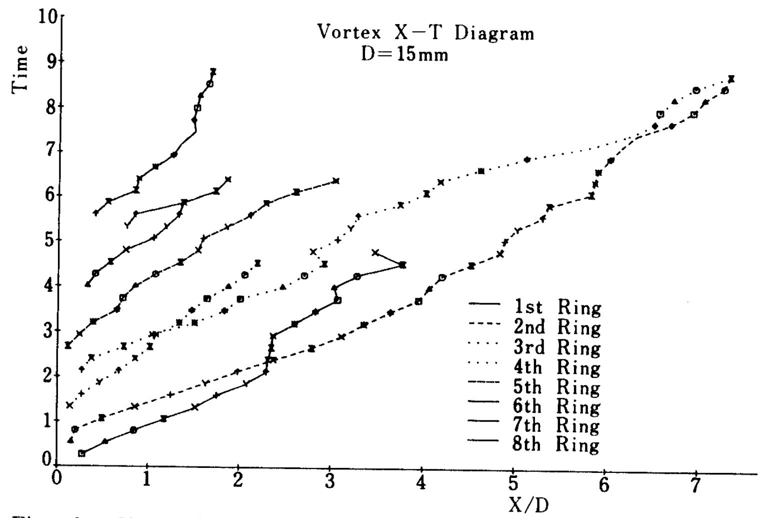

Fig. 6. $X-T$ diagram of a series of vortex rings. Vortices are interacted each other and make some pairs.

comparatively long valve opening time of 20 ms. In this case, the first and the second, the third and the forth, and the sixth and the seventh rings make up the pairs, respectively, and they play the passing game each other as a pair, then finally they merge into one turbulent vortex blob, as shown in the $X-T$ diagram of Fig. 6. Thus the so-called cascade process is realized and the mixture of the ejected and the entrained fluids proceeds as one big turbulent blob.

2.3 Elliptic vortex ring

The proceeding speeds of elements of the vortex filament consisting the elliptic vortex, are different due to the variation of the curvature of the filament. The element with the smaller curvature proceeds faster while the element with the larger one does

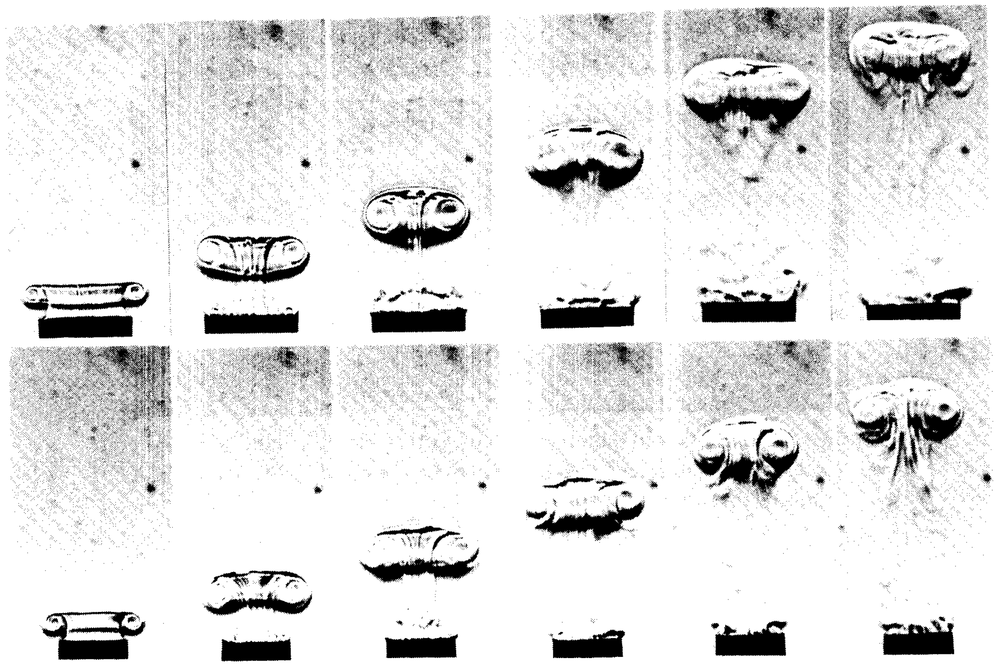

Fig. 7. A series of pictures from two directions showing the deformation of elliptic vortex ring. Upper half of each pair of the photographs shows the $X-Y$ plane and the lower half does the $X-Z$ plane at the same instant, respectively. Ratio of the major and minar radii is 1.5:1, $\Delta T=1$ ms, delay time $t=3$, 5, 7, 10, 13 and 16 ms.

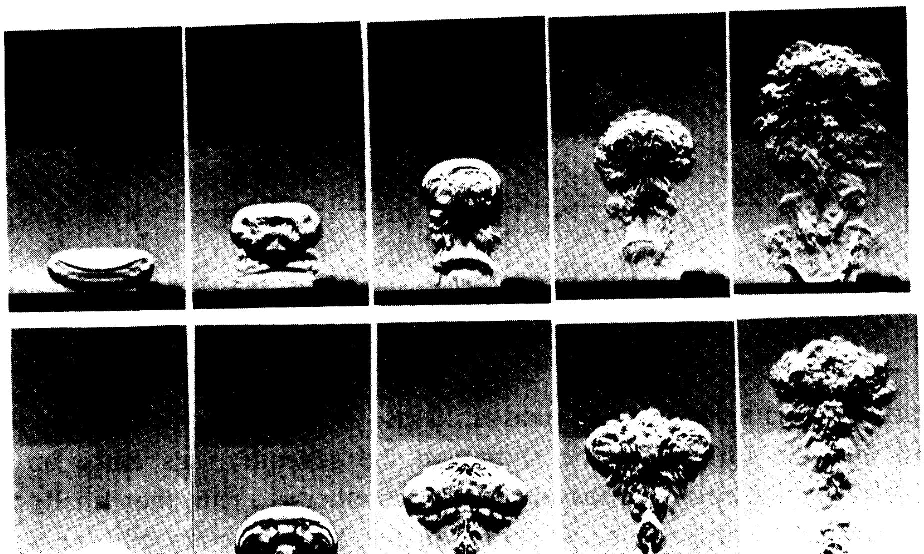

Fig. 8. A series of picture of elliptic vortex ring with the ratio of 4:1, $\Delta T=1$ ms, delay time $t=3$, 4, 5, 6 and 8 ms, respectively.

slowly in the perpendicular direction to the plane of the element. The deformation process of the ring repeats as the forward and backward bending motion of the major and the minor axes alternatively, and finally they approach to the flat circular ring due to the diffusion. Figures 7 and 8 are series of pictures taken from two directions, with the principal axis ratio of 1.5:1 and 4:1. The upper half shows the view in $X-Y$ plane and the lower half does that in $X-Z$ plane at the same instant, respectively. The ring element stretches in one direction with bending while it shrinks in the other direction. As the ratio of the principal radius increases, the tendency of the bending and stretching becomes stronger. Figure 9 is the daigram of $X-Y$ plane (fine line) and $X-Z$ plane (bold line) of one ring though the vortex filament is not straight as seen in pictures. In the figure, the same marks denote the positions of the major and minor axes of the same instant. As shown in the figure, the direction of the bending and the length of the lines are alternatively changed. As increasing the ratio of the principal radius, variations of the bending increase and enhance the transition to the turbulence.

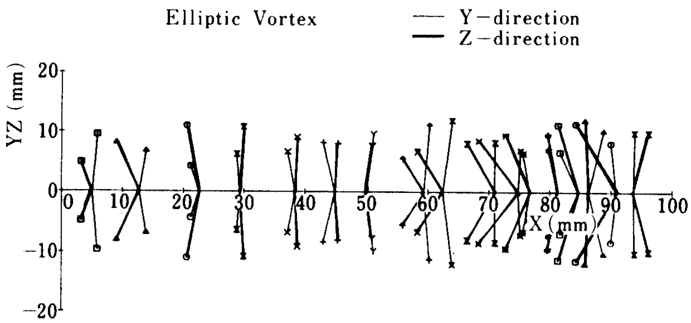

Fig. 9. $X-Y$ diagram (fine line) and $X-Z$ diagram (bold line) showing the deformation of elloptic vortex with the ratio of 4:1. The same marks denote the positions at the same instant.

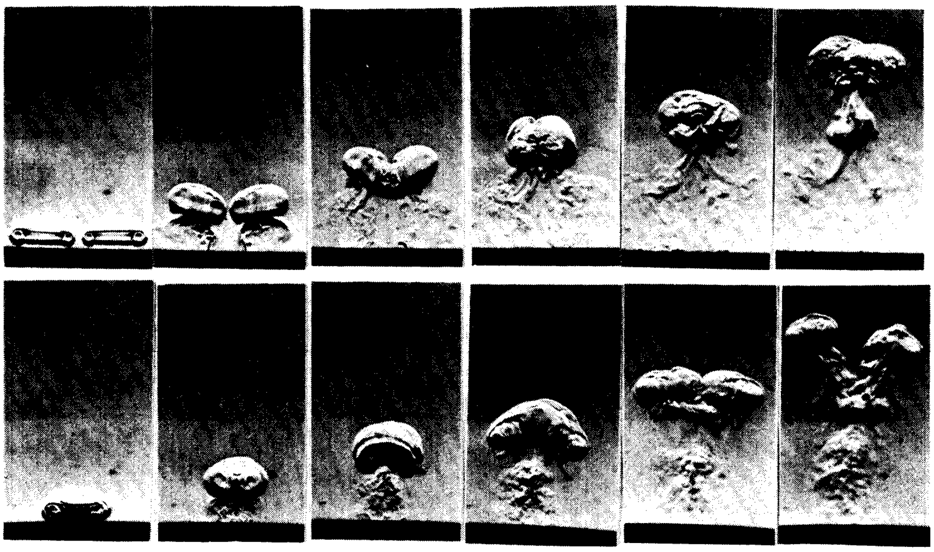

Fig. 10. A series of visualized picture from two directions showing the interaction of two vortex rings. Upper half of each pair of photographs show the $X-Y$ plane and the lower one does the $X-Z$ plane at the same instant, respectively. $D=13$ mm, distance $L=21$ mm, $\Delta T=2$ ms, $t=5$, 9, 13, 17, 23 and 30 ms.

2.4 Two parallel axis vortex rings

Figure 10 is a series of pictures taken from two directions, showing the interactions of two vortex rings ejected simultaneously from two identical orifices. The upper and the lower pictures show the view in the $X-Y$ plane and the $X-Z$ plane, respectively, at the same time instant. Two rings seen in the $X-Y$ plane become closer due to the induced velocity by the other one and they interact each other and merge into one distorted ring. Depending on the curvature of each element of the vortex filament, the distorted ring varies its shape, and splits into two rings in $X-Z$ plane after the second crosslinking. These phenomena are plotted on the $X-Y$, $X-Z$ diagrams in Fig. 11, in which two rings in the $X-Y$ plane merge into one and two overlapped rings in the $X-Z$ plane are split into two rings. The same mark denotes those of $X-Y$ plane (solid line) and $X-Z$ plane (broken line) taken at the same time instant and the length of the lines denotes the diameter of the vortex ring at that moment. When the distance between the two orifices is far, the rings interact weakly, and the crosslinking of the vortex filament does not occur. Contrary to this, when the distance between them is small, the strong interaction occurs within very short time, then after a turbulent blob remains as the mixture of the two rings. Furthermore, the process of the crosslinking also depends on the pressure of the gas bottle and the valve opening duration, which determine the intensity of the vortex filament. Even at the same distance from the two orifices, the phenomena of merging and splitting of two vortex rings are very sensitive to the surrounding condition; the typical merging and splitting are observed only within the narrow range of the parameters. Otherwise, the distorted ring after the crosslinking occurred travels along the axis while changing its form.

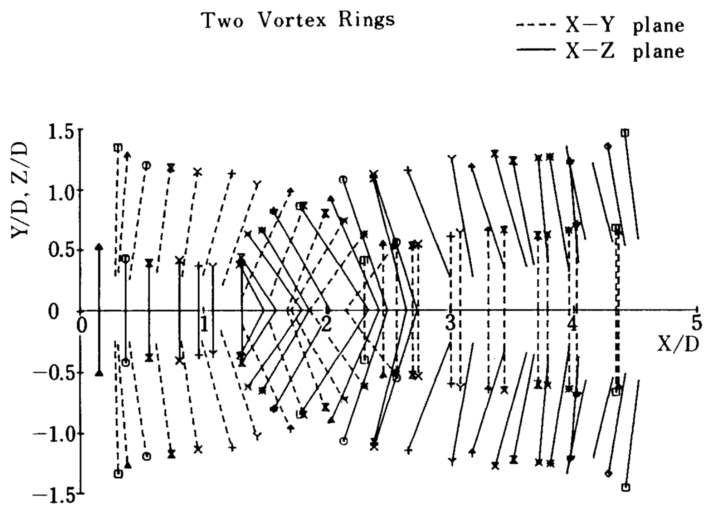

Fig. 11. Trajectories of the vortices ejected from two orifices, shown in Fig. 10. The vortex rings in $X-Y$ plane are denote broken lines, and those in $X-Z$ plane are by solid lines. The same marks show the position at the same instants.

§III. Numerical Simulation

For a numerical simulation of the interactions of co-axial vortex rings, the two dimensional vortex motion is considered for simplicity. Calculation is carried out for various conditions corresponding to the experiments using NEC 9801 micro-computer. The results of calculation are presented in the graphic display and the trajectories of the vortices are taken from the hard copy of the display. Also the motion of the filaments was recorded by 16 mm movie camera using single exposure mechanism. One vortex consists of seven vortex filaments with the same intensity and direction placing at a hexagon and center, and the distance of the nuscent filaments is R. One pair of the vortex blobs with the opposite direction is placed at the distance of two centers $D=10$ symmetrically along the axis. Initially, the vortex pairs are arranged at the distances based on the experimental data along the axis. As the time passes, each filament changes its position due to the mutual induced velocities of these vortex filaments. In order to be free from the numerical diffusion, forth order Runge-Kutta method is employed for the time integration. Figures 12 (a)-(c) are the trajectories of the vortex filaments ($X-Y$ diagram) using the different marks for the different blobs in the case of $R=1.5$ and $DT=0.1$, corresponding to the case of two, three and four sets of the vortex blobs. As each vortex filament moves its own trace, mixings with the other blobs are observed. As all the trajectories are shown in one figure, the positions of the filaments are overlapped, promiscuously. To clear the deformation of one of the vortex blobs, the time dependence of the vortex filament is shown in Figs. 13 (a)-(c) together with the trajectories of the centroid of each vortex blob for the case of four sets of vortex pair. From these figures, it is shown that each vortex blob is elongated and is twisted by the other blob to make one blob, and four sets of the vortex blob combined into two blobs, then finally they merge into one large blob, in which all of the filament are mixed. In these figures, upper half plane of the symmetrical axis are shown. This process seems to be in good agreement with the experiment. It is more clearly seen in Figs. 14 (a)-(c) as the $X-T$ diagram of the centroid of the blob in the case of $R=1.5$ corresponding to Fig. 12 (a)-(c), respectively.

On the other hand, as the distance R becomes small, the interaction of the filaments with the other blobs becomes weak, and these filaments keep their identity, and also if DT is small, mixing of the vortex filaments weakens due to the small numerical diffusion, and the results of simulation approach to that of the potential flow. Fig. 15 is one example of the vortex trajectories showing the two sets of vortex pair with the case of $R=0.5$ and $DT=0.05$. Alternations of the forward and the backward blobs are repeated as seen in the figure, though it is not realized in the experiments. Experimental process can be realized by suitably choosing the appropriate parameters, for example, R or DT and the number of vortex filaments in one blob.

§IV. Concluding Remarks

Three interaction phenomena of the vortex rings were carried out experimentally together with the numerical simulations of two dimensional case. The first is the mutual

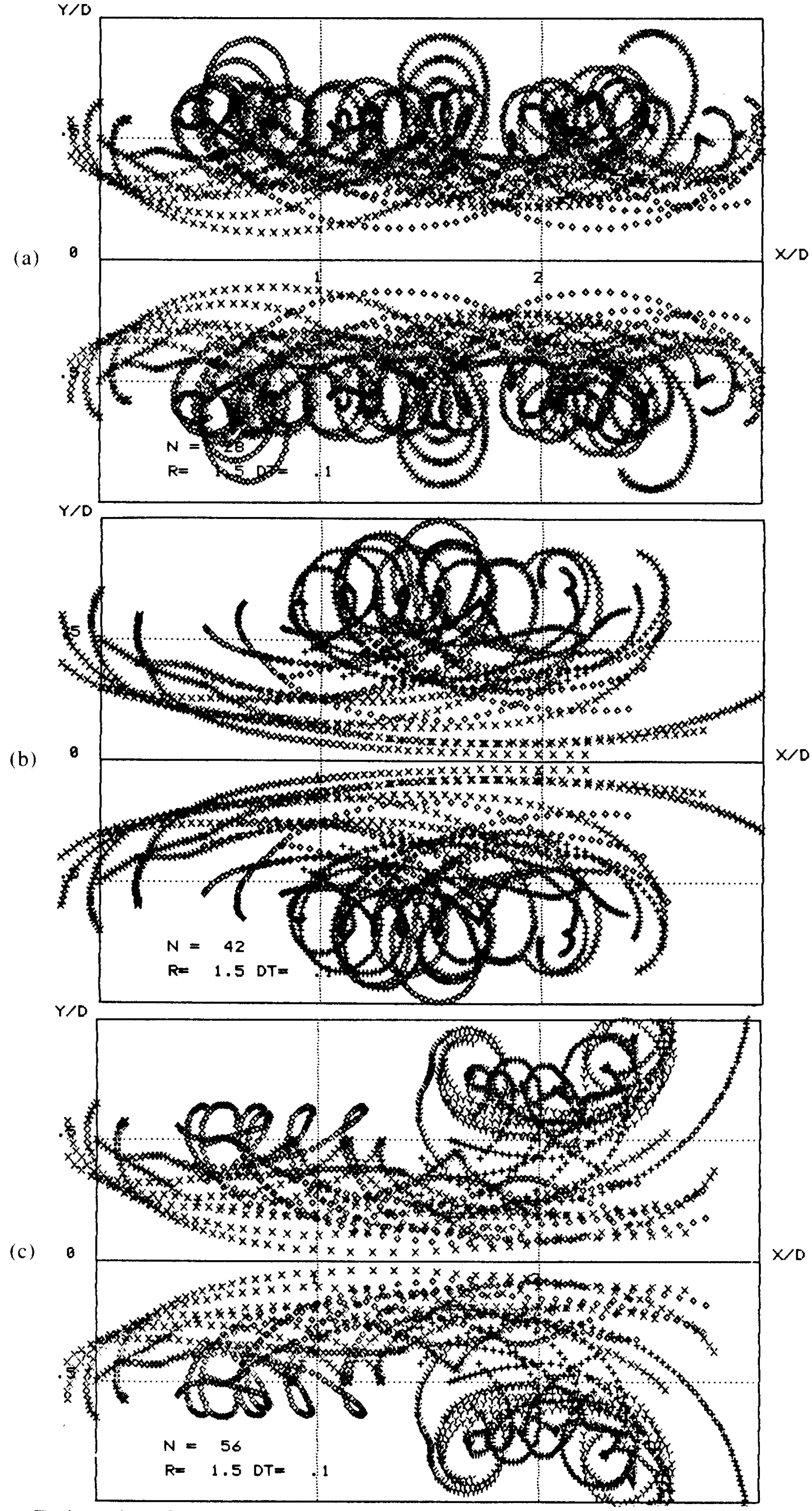

Fig. 12. Trajectories of vortex filaments calculated in two dimensional case by discrete vortex method. Same mark shows the filament of the same blob. Distance of vortex nuscent vortex R is 1.5, DT=0.1, respectively. (a) Two sets of vortex pair, total number of vortex filaments N=28. (b) Three sets of vortex pair, N=42. (c) Four sets of N=56.

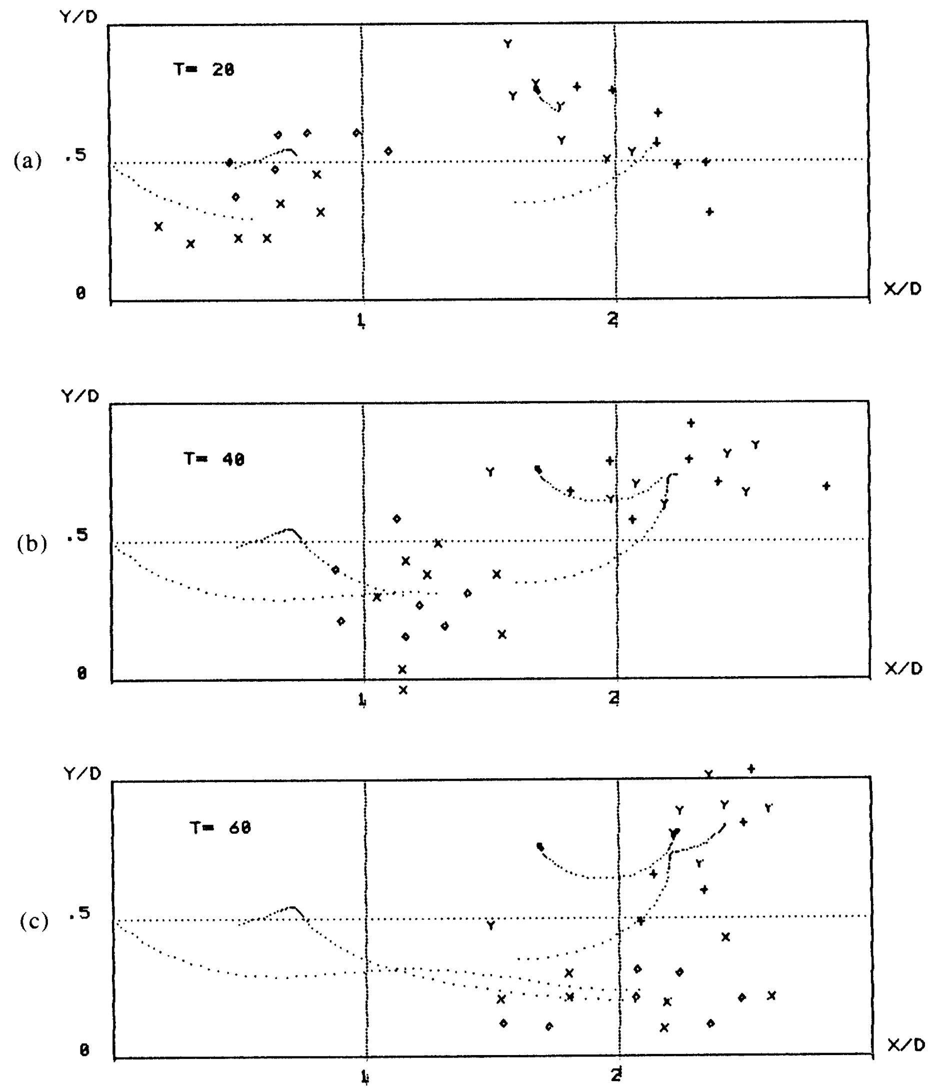

Fig. 13. Time dependence of vortex formation of four set of pair, corresponding to Fig. 12 (c). Upper half of the axis is shown. (a) time step $T=20$, (b) $T=40$, (c) $T=60$, respectively.

interaction of the succeeding vortex ring along an axis, and the other is the deformation of an elliptic vortex ring in which the interaction due to the vortex filament itself is considered. The last is the crosslinking and merging phenomena of two vortex rings.

The cascading, crosslinking and merging phenomena which are the elementary process in turbulent flow were realized in these simple examples. Substantial process of these interactions were explained qualitatively. Also, two dimensional numerical simulation using discrete vortex method shows good agreement with the experimental data, provided with the appropriate parameters.

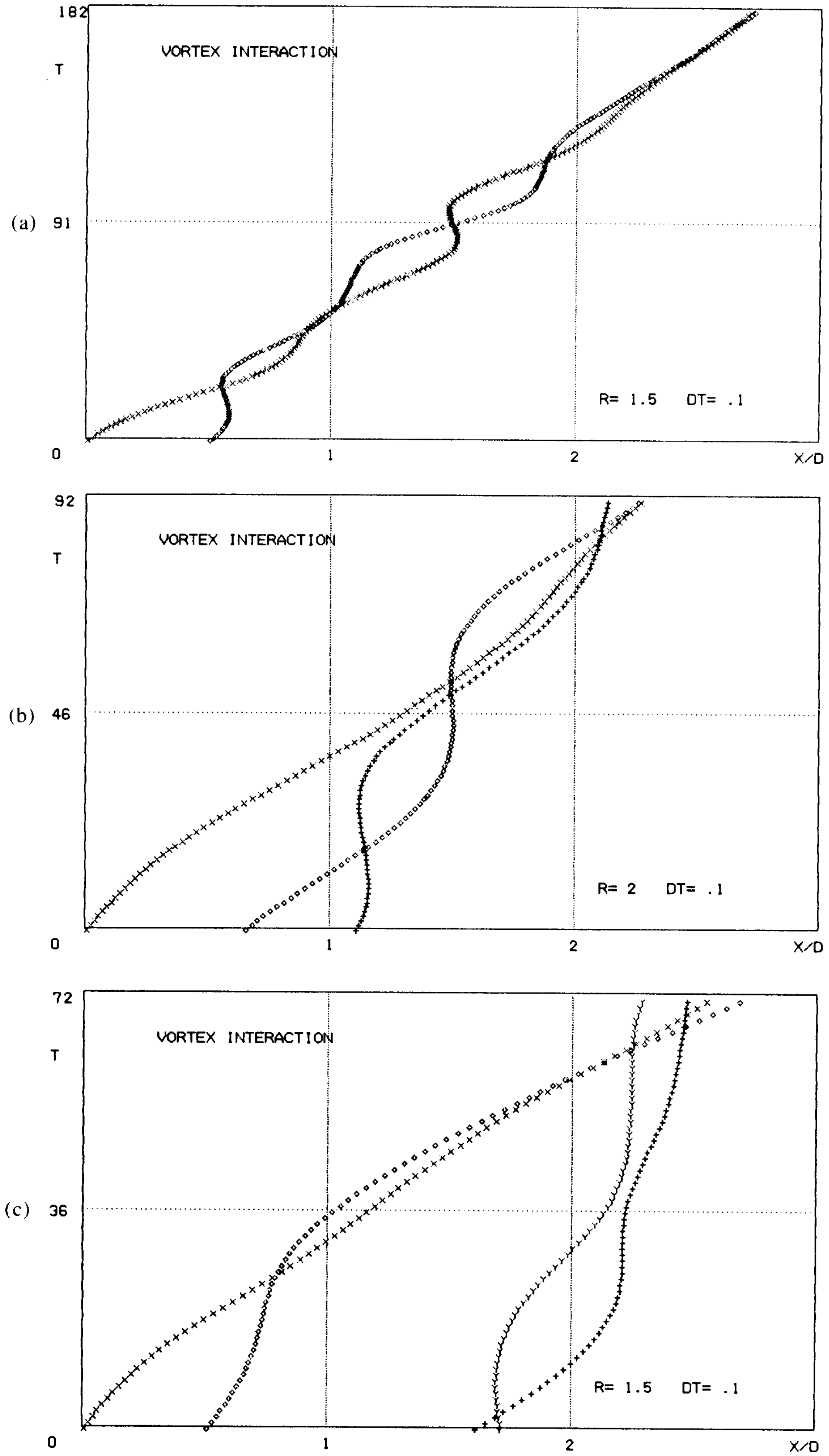

Fig. 14. $X-T$ diagram of the centroid of each vortex blob. $R=1.5$, $DT=0.1$. (a) Two sets of vortex pair, (b) three sets, (c) four sets.

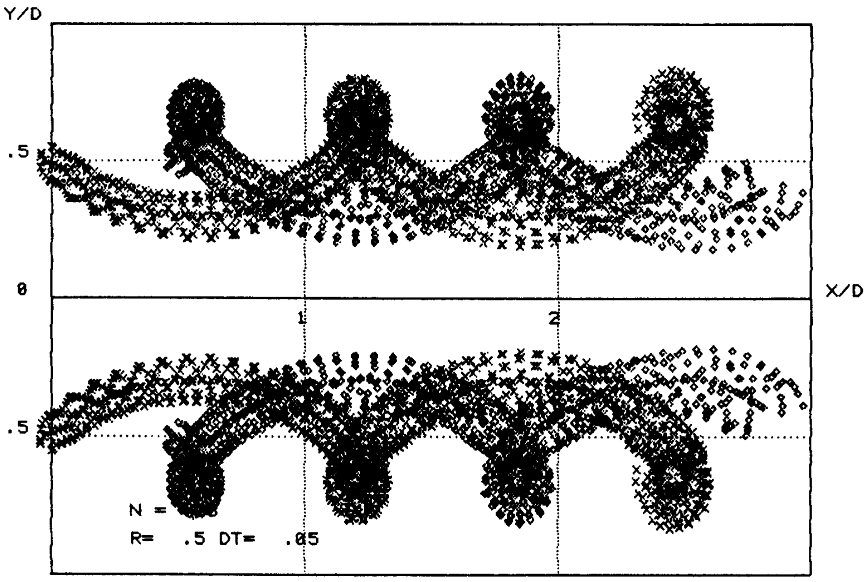

Fig. 15. $X-Y$ diagram of two sets of vortex pair, R=0.5, DT=0.05. The shape of blob is kept due to the small numerical diffusion.

REFERENCES

[1] Thomson, J. J.: A treatise on the motion of vortex rings, London, Macmillan (1983).
[2] Saffman, P. G.: The velocity of viscous vortex rings, Studies on Appl. Math. *49* (1971) 371.
[3] Norbury, J. A.: A family of vortex rings, J. Fluid Mech. *57* (1971) 417.
[4] Maxworthy, T.: The structure and stability of vortex rings, J. Fluid Mech. *51* (1972) 15.
[5] Widnall, S.: The structure and dynamics of vortex filaments, Ann. Review Fluid Mech. *7* (1975) 141.
[6] Kambe, T. & Oshima, Y.: Generation and decay of viscous vortex rings, J. Phys. Soc. Japan *38* (1975) 271.
[7] Oshima, Y. *et al.*: Interaction two vortex rings moving along a common axis of symmetry, J. Phys. Soc. Japan *38* (1975) 1159.
[8] Oshima, Y. & Asaka, S.: Interaction of two vortex rings moving side by side, Natural Science Rep. Ochanomizu Univ. *26* (1975) 31.
[9] Leonard, A.: Simulation of three dimensional separated flows with vortex filaments, Proc. 5th ICNMFD (1977) 280.
[10] Oshima, Y. & Asaka, S.: Interaction of two vortex rings along parallel axes in air, J. Phys. Soc. Japan *42* (1977) 708.
[11] Oshima, Y. & Asaka, S.: Interaction of multi vortex rings, J. Phys. Soc. Japan *42* (1977) 1391.
[12] Oshima, Y.: Head on collision of two vortex rings, J. Phys. Soc. Japan *44* (1978) 328.
[13] Yamada, H. & Matsui, T.: Mutual slip through of a pair of vortex rings, Phys. Fluids *22* (1979) 1245.
[14] Oshima, K. *et al.*: Sound emission from burning puff, Lecture Note in Physics, Springer-Verlag (1977) 219.
[15] Oshima, Y. *et. al.*: Unsteady mixing of turbulent vortex puffs with surrounding atmosphere, ISAS RN *67* (1978).
[16] Oshima, Y. & Kuwahara, K.: Experimental and numerical study of vortex interaction, AIAA paper-84-1546, (1984).